ELSEVIER

Palaeogeography, Palaeoclimatology, Palaeoecology 202 (2004) 309–329

PALAEO

www.elsevier.com/locate/palaeo

Global change in the Late Devonian: modelling the Frasnian–Famennian short-term carbon isotope excursions

Yves Goddéris [a,*], Michael M. Joachimski [b]

[a] *Laboratoire des Mécanismes et Transfert en Géologie, UMR 5563, CNRS-Université Paul Sabatier-IRD, Toulouse, France*
[b] *Institute of Geology and Mineralogy, University of Erlangen-Nürnberg, Erlangen, Germany*

Received 7 June 2002; received in revised form 8 August 2003; accepted 12 September 2003

Abstract

A model of the global biogeochemical cycles coupled to a energy-balance climate model (the COMBINE model) is used to identify the causes of two large $\delta^{13}C$ value excursions across the Frasnian–Famennian (F-F) boundary. We test a scenario that links the sea-level rise to stratification of the Proto-Tethys ocean through the formation of warm saline deep waters in extended epicontinental seas. Even though this scenario can produce dysoxia below 100 m depth, it fails to increase the global burial flux of organic carbon and thus seawater $\delta^{13}C$ values, since stratification of the ocean leads to decreased productivity in surface waters. Several scenarios postulating a continental origin of the perturbations in the Late Devonian biogeochemical cycles are then tested. We found that weathering of platform carbonates exposed during the Early Famennian sea-level fall can account for a maximum positive shift in $\delta^{13}C$ value of +0.7‰ at the end of the sea-level fall episode. Another +1.0‰ increase in $\delta^{13}C$ might originate from rapid spreading of vascular land plants near the F-F boundary, postulating that higher plants globally increased the weatherability of continental surface, and that colonized continental area increased by 30% across the F-F boundary. Finally, the $\delta^{13}C$ excursion observed at the base of Upper *rhenana* Zone and the rapid increase of the carbon isotope ratios at the F-F boundary require an increase of phosphorus delivery to the ocean by 40%, coeval with the sea-level rises. Once the calculated $\delta^{13}C$ values are in agreement with the measured data, the COMBINE model calculates a decrease in atmospheric pCO_2 from pre-perturbation 2925 ppmv in the Lower *rhenana* conodont Zone to 1560 ppmv in the Upper *triangularis* Zone. This decrease in pCO_2 is due to the increase in burial of organic matter during the Kellwasser events, and increased continental weatherability triggered by the spreading of continental vascular plants. These changes occur within 4 million years. The corresponding global climatic cooling reaches 4.4°C at the pole, and 2.1°C at the equator.

Keywords: modelling; carbon dioxide; seawater; isotope ratios; Frasnian; Famennian

1. Introduction

The Late Devonian faunal crisis represents one of the most prominent mass extinction events in

* Corresponding author. Tel.: +33-5-6155-6841; Fax: +33-5-61-55-61-13.
E-mail addresses: godderis@lmtg.ups-tlse.fr (Y. Goddéris), joachimski@geol.uni-erlangen.de (M.M. Joachimski).

0031-0182/03/$ – see front matter © 2003 Elsevier B.V. All rights reserved.
doi:10.1016/S0031-0182(03)00641-2

Earth history, affecting preferentially low-latitude tropical shallow water ecosystems. This crisis lasted 1–3 million years with a major extinction pulse at the Frasnian–Famennian (F-F) boundary. The causes of this mass extinction have been widely discussed in the literature (for a review see Hallam and Wignall, 1997). Based on various qualitative scenarios, the extinction has been attributed to global anoxia (Buggisch, 1991; Joachimski and Buggisch, 1993; Murphy et al., 2000), climate warming (Thompson and Newton, 1988; Ormiston and Oglesby, 1995), climate cooling (Copper, 1977, 1986; Joachimski and Buggisch, 2002), the spreading of land plants (Algeo et al., 1995), intensified tectonic activity (Racki, 1998), and single or multiple bolide impacts (McLaren, 1970; McGhee, 2001).

Coincident with this crisis are two periods of enhanced sedimentation of organic matter (Kellwasser horizons) that accumulated under dysoxic to anoxic conditions (Joachimski and Buggisch, 1993). Both periods of enhanced organic carbon burial correspond to major positive excursions of +3‰ in global surface water $\delta^{13}C$ values (Joachimski et al., 2002). The first excursion coincides with a minor short-term rise in sea level (Fig. 1). The onset of the second excursion is observed within the latest Frasnian and also correlates with a sea-level rise. However, a prominent sea-level fall is observed in the earliest Famennian with the $\delta^{13}C$ record still displaying high values until the base of the Upper *triangularis* conodont Zone, (Joachimski and Buggisch, 1993; Joachimski et al., 2001, 2002).

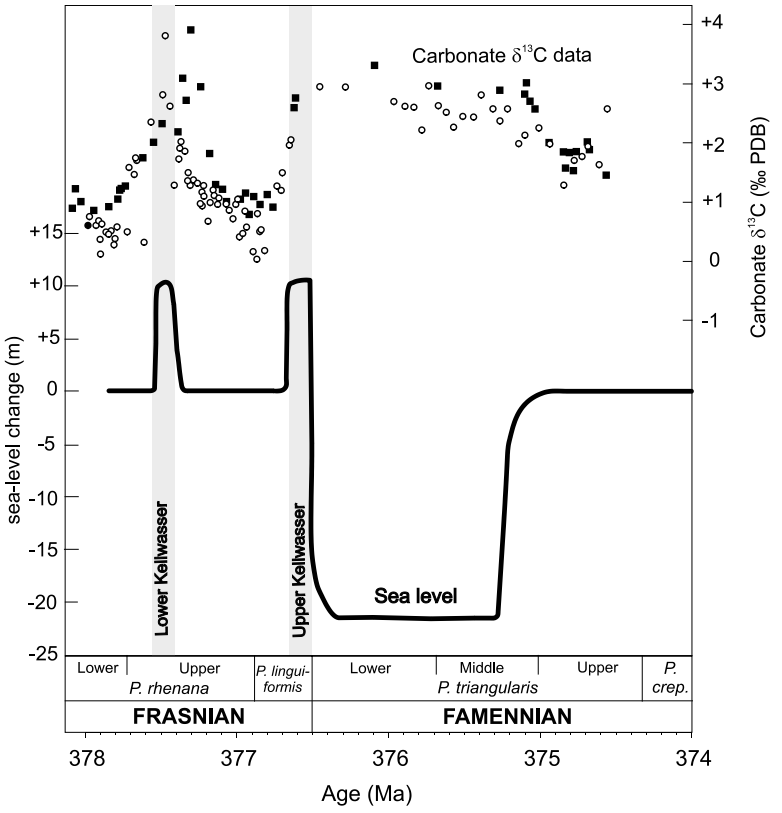

Fig. 1. Carbonate $\delta^{13}C$ value record measured across the F-F boundary in the Steinbruch Schmidt (open circles) and Benner (squares) sections (Joachimski and Buggisch, 1993) in comparison to changes in sea level (Johnson et al., 1985). Lower and Upper Kellwasser horizons are represented by the gray bars. Minor difference in the timing of the lower carbon isotope excursions is based on the assumption of constant sedimentation rate.

The duration of the positive carbon isotope anomalies is estimated using the Devonian time scale of Tucker et al. (1998) and assumptions concerning the relative duration of individual conodont zones from Sandberg and Ziegler (1996). The durations of the Upper *Palmatolepis rhenana*, *Palmatolepis linguiformis* and Lower *Palmatolepis triangularis* conodont Zones are estimated to be 850, 360 and 730 kyr, respectively. Knowing the thickness of sediments deposited during the respective conodont zones and assuming constant sedimentation rates, the durations of the $\delta^{13}C$ value anomalies are estimated to be around 0.5 Myr (base of the Upper *rhenana* Zone) and 1.2–1.8 Myr (F-F transition). Given the response time of carbon within the ocean–atmosphere system ($\sim$200 000 years, François and Goddéris, 1998), such big and short $\delta^{13}C$ value excursions probably correspond to major perturbations of the carbon geochemical cycle. Interestingly, oxygen isotope ratios measured on conodont apatite show two positive excursions of +1.5‰ that parallel the positive excursions in $\delta^{13}C$ values (Joachimski and Buggisch, 2002). Calculated paleotemperatures indicate significant climatic cooling of the low latitudes of 5–7°C, potentially as a consequence of the perturbations in the carbon geochemical cycle.

The aim of this study is to quantify the main biogeochemical fluxes across the F-F boundary and to model the imprint on global climate. Since the only available quantitative time series that recorded environmental changes across the F-F boundary are the measured carbonate $\delta^{13}C$ and $\delta^{18}O$ values, any scenario of the evolution of the global carbon–alkalinity cycles must be in agreement with those quantitative data. We thus build and use a numerical model of the carbon, alkalinity, oxygen and phosphorus biogeochemical cycles, coupled to a 1-D energy-balance climate model (the COMBINE model) to explore the validity of the various proposed scenarios for the F-F interval. The model calculates the $\delta^{13}C$ values of all the exospheric carbon boxes and the output is compared to measured values from one scenario to the other. Once agreement between calculated and measured $\delta^{13}C$ data has been reached, we have some confidence in the calculated evolution of the content of the various reservoirs (for instance, the atmospheric pCO_2) and in the calculated evolution of global climate.

2. The COMBINE model

2.1. General structure

The COMBINE model (COupled Model of BIogeochemical cycles aNd climatE) (Fig. 2) is an atmosphere–ocean geochemical model fully coupled to a simple 1-D climatic model. To reproduce the Late Devonian geographic configuration, we divide the ocean into two major oceanic basins, the Panthalassa and the Proto-Tethys oceans (Scotese and McKerrow, 1990). The respective areas of the two basins are estimated from Devonian paleogeographic maps to be 355×10^6 km^2 for the Panthalassa and 53×10^6 km^2 for the Proto-Tethys ocean. Another geographical configuration might be computed for other continental configurations corresponding to other events in the geological past. This geographical partitioning is required because most of the isotopic data were measured on sections deposited on the margins of the Proto-Tethys ocean and since the response to any perturbation of this oceanic basin might be potentially different from the response of the Panthalassa ocean. Both oceanic basins are divided into five boxes. The open oceans include the photic zone (0–100 m depth), a thermocline reservoir (100–1000 m depth) and a deep sea reservoir (1000–5000 m depth). Two epicontinental reservoirs are added for both basins: a surface epicontinental box, ranging from 0 to 100 m, and a deep epicontinental box (100–200 m depth). These two boxes represent the shallow epicontinental seas. The atmosphere is described by one box. Elements may be added to or removed from the ocean–atmosphere system due to chemical weathering of the continents and the input by volcanic degassing, and through deposition on the seafloor.

The geochemical model is coupled to an energy-balance climatic model developed by François and Walker (1992) that has been previously used and validated for several paleoclimatic studies

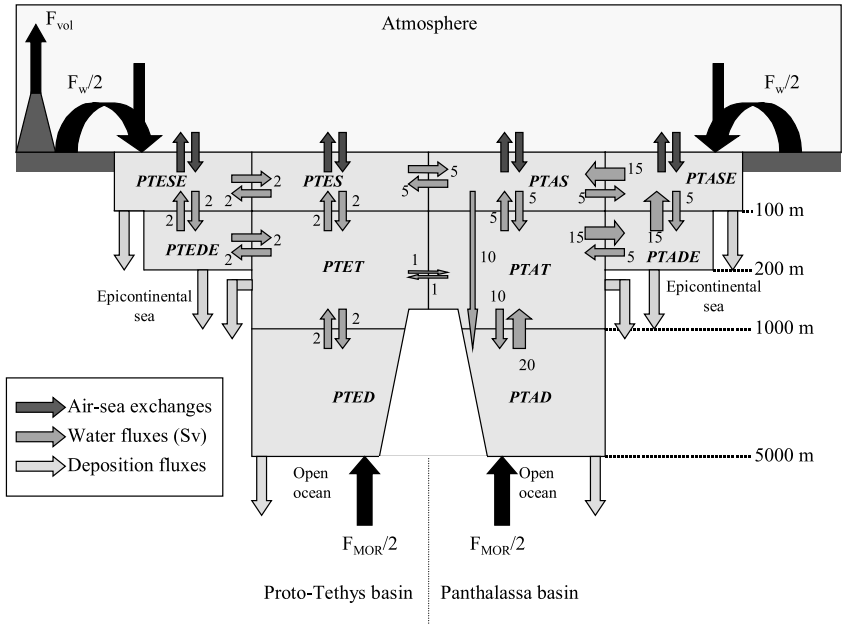

Reservoir acronyms:	Proto-Tethys	Panthalassa
Epicontinental surface (0-100 m)	PTESE	PTASE
Epicontinental deep (100-200 m)	PTEDE	PTADE
Open ocean surface (0-100 m)	PTES	PTAS
Open ocean thermocline (100-1000 m)	PTET	PTAT
Open ocean deep (1000-5000 m)	PTED	PTAD

Fig. 2. A schematic view of the COMBINE model. The global ocean is divided into two oceanic basins. The Proto-Tethys basin is the smallest one. The carbon, alkalinity, oxygen and phosphorus contents are calculated for each box at each time step of the integration. The black arrows represent the transfer of elements through geological processes: continental weathering and degassing through volcanoes and mid-ocean ridge systems.

(François and Walker, 1992; Goddéris and François, 1995; Veizer et al., 2000). It calculates at each time step the mean air temperature in 18 latitude bands as a function of (1) the model atmospheric CO_2, (2) the latitudinal distribution of Devonian continental masses, and (3) Devonian solar luminosity (98% of the present-day solar luminosity; Endal and Sofia, 1981). The meridional heat flux is divided into the sensible, latent, and oceanic components. The sensible and oceanic heat transfer coefficients are made dependent on latitude. Today, these coefficients are lower over the South Pole compared to their values around the North Pole. This particular configuration is the result of the existence of circumpolar atmospheric and oceanic currents along Antarctica. We choose to keep the heat transfer coefficients identical to modern values in order to reproduce a colder and drier climate at the South pole, where the Gondwana continent was located, than at the North pole, itself free of continental mass.

The water fluxes between the oceanic boxes are prescribed. Only a rough pattern of the Devonian oceanic circulation can be estimated. Based on the fact that the seaways between the Proto-Tethys and the Panthalassa basins were apparently restricted to continental platforms (Scotese and McKerrow, 1990), we assume weak to no horizontal exchange between the thermocline and deep reservoirs of both basins (respectively 1 and 0×10^6 m^3/s). The exchange through the

open ocean surface reservoir is fixed to 5×10^6 m^3/s. We furthermore assume that the vertical circulation in the Panthalassa ocean can be described by the upwelling of waters from the thermocline reservoir into the epicontinental reservoirs, compensated by the sink of surface waters directly from the open ocean surface reservoir into the deep ocean reservoir. The input of well-oxygenated surface waters directly into the deep sea reservoir results in a steady-state oxygen concentration higher in the deep reservoir than in the thermocline reservoir. The Panthalassa ocean can thus be compared to the modern global ocean. On the other hand, we assume a simple mixing between all the boxes of the Proto-Tethys reservoir, without strong upwelling, a hypothesis that appears reasonable regarding the setting of the Proto-Tethys basin (Ormiston and Oglesby, 1995). Furthermore, we assume no input of surface waters directly into the deep ocean, leading to the location of an oxygen minimum zone in the deep reservoir, below 1000 m. The Proto-Tethys basin can thus be seen as a huge lake, relatively stratified, with less oxygenated conditions as depth increases.

2.2. Geochemical cycles

The model includes geochemical cycles for carbon, phosphorus (which is the only nutrient modelled), alkalinity and oxygen. The amount of carbon in the atmospheric reservoir is calculated by solving at each time step the differential equation describing the atmospheric carbon budget. The inputs are the subaerial degassing by volcanism (held constant at the 3.0×10^{12} mol/yr value), and the CO_2 degassing of the surface ocean, while the outputs are the consumption of atmospheric CO_2 by chemical weathering of carbonate and silicate rocks, and the dissolution of CO_2 in surface waters. The consumption of atmospheric CO_2 by silicate weathering is a linear function of continental runoff and land area, and a non-linear function (exponential) of the mean air temperature as well as of atmospheric CO_2 content (François and Walker, 1992). Because of this non-linearity, the use of global mean air temperature above continental areas in order to calculate the global silicate weathering rate is not rigorous. We thus follow an approach similar to François and Walker (1992) and Goddéris and François (1995) by dividing the Earth into 18 latitude bands, and using the mean zonal air temperature calculated for each latitude band by the climate model to estimate the zonal silicate weathering flux. All the terms are then added up to provide the global flux:

$$F^{w}_{sil}(t) = k_{sil}\times\sum_{j=1}^{18}\left[\mathrm{area}_j(t)\times\mathrm{runoff}_j(t)\times \exp\left(\frac{T_j-288.15}{10.95}\right)\right]\times FCO_2\times f_e \quad (1)$$

where k_{sil} is a constant, $\mathrm{area}_j(t)$ and $\mathrm{runoff}_j(t)$ are respectively the continental area and runoff at any time step in the latitude band j, and T_j is the mean air temperature in the latitude band j. The factor 10.95 assumes an activation energy of about 63 000 J/mol for the dissolution of silicates (Brady, 1991). The zonal continental runoff is estimated using the parameterization developed by François and Walker (1992), as a function of zonal temperature, latitude and the fraction of continental surface in each latitude band. FCO_2 represents the direct dependence of weathering on atmospheric pCO_2. In the absence of vegetation, this factor equals the atmospheric CO_2 (expressed in PAL) raised to the power 0.5 (Berner, 1994). In the presence of higher plants, this factor is calculated as follows (Berner, 1994):

$$FCO_2 = \left(\frac{2pCO_2}{1+pCO_2}\right)^{0.4} \quad (2)$$

We assume that, prior to the F-F perturbation, an arbitrary 10% of the continental area was covered with higher vegetation. The mean FCO_2 factor for each latitude bands is calculated as a linear mixing between non-vegetated and vegetated area values, weighted by the areas. f_e is a factor introduced by Berner (1994) that considers an expected enhancement of chemical weathering due to the presence of higher land plants (concentration of organic acids in soil, presence of microbes, development of roots). This factor is normalized to its present-day value. Following Berner (1994), f_e is set to 0.15 for non-vegetated areas, and to 0.75

for areas covered by gymnosperms. Each zonal mean f_e is calculated as the weighted FCO_2 value.

The same approach is adopted for the calculation of the consumption of atmospheric CO_2 by carbonate rock weathering F^w_{carb}, which is assumed to be a non-linear function of the continental runoff (François and Walker, 1992):

$$F^w_{carb}(t) = k_{carb} \times \sum_{j=1}^{18} (\text{area}(t) \times \sqrt{\text{runoff}_j(t)}) \times FCO_2 \times f_e \quad (3)$$

where k_{carb} is a constant. FCO_2 represents the atmospheric CO_2 dependence of the carbonate weathering, and is equal to the same FCO_2 factor used in the silicate weathering calculation (Berner, 1994).

The amount of total dissolved inorganic carbon (DIC) and alkalinity for each oceanic box is calculated at each time step by solving the differential equation describing its budget. Depending on the box (Fig. 2), the inputs are the CO_2 degassing at mid-ocean ridge systems into the deep ocean (global value kept constant at 1.5×10^{12} mol/yr), the supply of carbon and alkalinity by continental weathering, the DIC and alkalinity flux transported by water fluxes into the ocean, the oxidation of the sinking organic matter from the photic zone into the deeper parts of the ocean, and the dissolution of atmospheric CO_2 into the ocean. The outputs are represented by the flow of DIC and/or alkalinity out of the box by transport, by the consumption of carbon by biological activity within the photic zone, by deposition of carbonate and of organic carbon, and degassing of CO_2 to the atmosphere.

The complete carbonate speciation, including the calculation of pH, $[H_2CO_3]$, $[HCO_3^-]$, $[CO_3^{2-}]$ as a function of the salinity and temperature of the oceanic reservoir, and of the partial pressure of dissolved CO_2, is then calculated in each oceanic box, once their respective DIC and total alkalinity content are calculated by solving the differential system. The intermediate depth and deep sea temperatures are fixed to 276 K, while the surface temperature of the Panthalassa basin is calculated as the mean global air temperature at the surface estimated by the climate model. The Proto-Tethys sea surface temperature is calculated as the mean air temperature between 10°S and 10°N. The air–sea CO_2 exchange between the surface oceanic box i and the atmosphere is estimated as follows:

$$F_{atm-i}(CO_2) = K_0 \times \left(pCO^{atm}{}_2 - pCO^i_2\right) \times \text{area}_i \quad (4)$$

where K_0 is a constant (Sarmiento et al., 1992), pCO_2^{atm} is the partial pressure of atmospheric CO_2, pCO_2^i is the partial pressure of dissolved CO_2 in reservoir i, and area_i is the reservoir area at the surface.

The calcium budget calculated for each oceanic box allows the determination of the concentration of Ca^{2+}. The inputs to the ocean are the weathering of continental silicate and carbonate rocks, while the output is the accumulation of carbonate on the seafloor. There is no convincing evidence for the existence of calcareous phytoplankton in the Paleozoic. For this reason, we assume that the only precipitation of carbonate occurs on the continental shelves as shallow water carbonates, deposited above 100 m water depth. The carbonate accumulation flux is calculated following Opdyke and Wilkinson (1988):

$$F^d_{carb} = k_d \times \text{area}100_i \times (\Omega_{calcite} - 1)^{1.7} \quad (5)$$

where $\Omega_{calcite}$ is the calculated saturation ratio for calcite, k_d is a constant and $\text{area}100_i$ is the horizontal area above 100 m depth for the epicontinental surface reservoir i, calculated by the hypsometric module of the model (see Section 2.3).

The production of organic carbon occurs within the photic zones of both oceanic basins. The biological productivity is made proportional to the phosphorus input into the photic zones. This productivity flux feeds a particulate organic carbon reservoir (Petsch and Berner, 1998). The C:P value of the productivity flux is fixed to 117:1 (Anderson and Sarmiento, 1994). Dissolved phosphate is removed from the surface reservoir and incorporated into a particulate phosphorus reservoir. Particulate organic carbon and phosphorus then sink within the thermocline reservoir if they originated from the open ocean photic zone, or towards the sediment or deep epicontinental reservoir if they originated from the surface epicon-

tinental reservoir. Recycling occurs within the water column. The recycling rate is a linear function of the dissolved oxygen content above 5×10^{-3} μmol/kg O_2. Below this value, anoxic recycling is assumed to occur at a constant rate. The model includes a simplified sediment module in order to estimate the amount of organic carbon and phosphorus that is buried relative to the amount that reaches the sediment, the difference being recycled (François and Walker, 1992; Goddéris, 1997). This model includes a sediment mixed layer where organic matter is oxidized by oxygen, and a sulfate reduction layer below it. Since no sulfur cycle is included in this model, the concentration of sulfate within the deepest sediment layer is assumed to be constant. The C:P ratio of the buried organic matter is made dependent on the dissolved oxygen level within the water in contact with the sediment, increasing if the degree of anoxia increases (Van Cappellen and Ingall, 1996).

Phosphorite mineral precipitation, P sorption and iron coprecipitation are assumed to occur indistinctly within all oceanic reservoirs in contact with the seafloor. The corresponding removal of phosphorus is made proportional to the dissolved phosphate content of the respective reservoir. An additional sink of phosphorus is represented by the scavenging of phosphorus by ferric oxyhydroxides formed within hydrothermal systems. This process occurs within the deep oceanic reservoir of both the Panthalassa and Proto-Tethys oceans, and is assumed to be proportional to the hydrothermal activity (kept constant in all simulations), and to the dissolved phosphate concentration of the deep reservoirs (Benitez-Nelson, 2000). The supply of phosphorus from continental rock weathering is modelled as a function of continental runoff and vegetation in the same way as continental carbonate weathering. Under present-day conditions, the weathering input of P into the ocean reaches 45.0×10^9 mol/yr (Petsch and Berner, 1998).

At the time scale of the present study, the source of oxygen is thus the burial of organic matter, while the sink is the oxidation of old sedimentary reduced carbon (SRC) exposed on the continents. The oxidation of old SRC is assumed to be dependent on the continental runoff in the same way as the weathering of continental carbonates (François and Walker, 1992):

$$F^{w}_{SRC}(t) = k_{SRC}\times\sum_{j=1}^{18}\left(\mathrm{area}_j(t)\times\sqrt{\mathrm{runoff}_j(t)}\right) \quad (6)$$

where k_{SRC} is a constant. The crustal carbon released during the oxidation of the SRC is transported to the ocean, and constitutes a source of inorganic carbon for the ocean.

In order to increase the time step of the calculation, the partial pressure of oxygen in surface waters is assumed to be instantaneously at equilibrium with the atmospheric O_2 pressure. The surface water concentration of dissolved oxygen is then calculated as a function of the partial pressure in water, salinity and temperature of surface waters using the Wanninkof (1992) formalism.

The COMBINE model includes a ^{13}C cycle. The exchange of CO_2 between the various surface ocean boxes and the atmosphere occurs with an isotope fractionation, through the exchange equation derived by Munhoven (1997):

$$f_{oc-atm} = K_0\times(\phi_{as}\times pCO^{atm}{}_2 - \left(\delta^{13}C_i - \delta^{13}C_{atm} + \phi_{sa}\right)\times pCO^{i}_{2})\times \mathrm{area}_i \quad (7)$$

where f_{oc-atm} represents the net carbon isotope exchange between the atmosphere and the oceanic surface reservoir i (positive if the net flux is from the ocean towards the atmosphere), $\delta^{13}C_i$ is the $\delta^{13}C$ value of DIC in surface ocean reservoir i, and $\delta^{13}C_{atm}$ is the atmospheric $\delta^{13}C$ value. ϕ_{as} and ϕ_{sa} equal respectively $\alpha_{as}-1$ and $\alpha_{sa}-1$, where α_{as} and α_{sa} are the one-way fractionation factors. ϕ_{as} and ϕ_{sa} are fixed to -0.002 and -0.010 (Siegenthaler and Münnich, 1981). The $\delta^{13}C$ value of each DIC species is calculated for each oceanic reservoir. The fractionation between dissolved CO_2 and bicarbonate, and between bicarbonate and carbonate ion is calculated as a function of temperature (Mook et al., 1974; Freeman and Hayes, 1992) in each oceanic box. The biological isotope fractionation occurring during the formation of particulate organic carbon in the photic zone is calculated for each reservoir as a function of dissolved CO_2 and PO_4^{3-} (Kump and Arthur, 1999), and dissolved oxygen (Berner et

al., 2000). Carbonate precipitation is assumed to occur without fractionation. The $\delta^{13}C$ values of continental SRC and continental carbonates are respectively fixed at −28‰ (Hayes et al., 1999) and +1‰ PDB (excluding the carbonate platforms exposed during the Famennian sea-level fall, see below). The $\delta^{13}C$ of the carbon degassed along mid-ocean ridges is set at the mantle value of −5‰ PDB (Holser et al., 1988). The $\delta^{13}C$ value of subaerial volcanism is the result of the mixing of mantle-originated carbon, carbon from recycled carbonates (including alteration products of seafloor basalts) and sedimentary organic carbon at subduction zones (Wallmann, 1999). The respective contributions of these three terms are not known (Goddéris and Veizer, 2000; Deines, 2002). The $\delta^{13}C$ value of subaerial volcanism is here set at a constant −1‰ PDB for calibration reasons, thus assuming a mixing between mantle carbon and carbon degassed from subducting carbonates in agreement with Caldeira (1992) and Goddéris and François (1996).

Finally, the salinity of each reservoir is calculated. Since isolated seas are assumed to be part of the model epicontinental reservoirs, these reservoirs should display a higher salinity than the open ocean reservoir. We thus force an evaporation minus precipitation budget to positive values for the epicontinental reservoirs, and to negative values for open ocean surface reservoirs in such a way that the global water mass is held constant. This disequilibrium is a function of the epicontinental sea surfaces, increasing when the surface of epicontinental seas increases (during sea-level rises). In the ocean, salinity is transported by the water fluxes. At steady state, this procedure leads to a salinity ranging from 34.5‰ for the Proto-Tethys open surface reservoir (PTES) to 37‰ for the small surface epicontinental reservoir of the Proto-Tethys basin (PTESE). The global mean salinity is fixed to a constant value of 35‰.

2.3. Sea-level changes

The sea-level curve (Johnson et al., 1985) is a qualitative reconstruction (Fig. 1). The exact amplitudes of the sea-level changes are not known. However, these are second-order sea-level changes, and their amplitude most probably lies between 1 m and several tens of meters. Here, we assume two sea-level rises of 10 m each, while the sea-level fall during the Early Famennian is assumed to be 20 m. There are good indicators that the two sea-level rises are not glacio-eustatic fluctuations, since there is no evidence for the existence of a continental ice cap that could fluctuate in volume prior to the end of the Frasnian. On the other hand, these two transgressions are too rapid to be induced by variations in the volume of the mid-ocean ridge system. Since the mechanism for these sea-level rises is uncertain (Johnson et al., 1985), and in order to maintain the amount of water constant in the system, we simply model the two sea-level rises by artificially pushing up the deep seafloor. Regarding the Early Famennian sea-level fall, there is only vague evidence for the development of a hypothetical ice sheet, responsible for the sea-level drop (Streel et al., 2000). We will not take this into account, simply assuming an artificial deepening of the deep seafloor, to produce a sea-level fall at constant water volume. Since our goal is to study the impact of these fluctuations on the geochemical cycles, the exact mechanism that produces these sea-level rises and falls is of secondary importance, as long as the causes of these fluctuations do not imply directly geochemical fluxes (such as degassing of CO_2, or changes in the weatherability of continental surfaces following the development of continental ice sheets). The lack of constraints on the causes of the sea-level fluctuations leads us to neglect these possibilities. The expected impacts of sea-level change on the geochemical cycles as described by the COMBINE model at the million year time scale are as follows:

(1) The consecutive change in continental area will directly influence the discharge of elements produced by chemical weathering of continental rocks. This effect is quantified within the model, through the hypsometric module which estimates the continental area flooded during sea-level rise or exposed during sea-level fall. This module calculates the volume and horizontal surfaces for all oceanic boxes, through simple geometric considerations, as a function of sea level.

(2) A sea-level rise or fall will change the volume and surface of the oceanic reservoirs and affect evaporation as well as continental precipitation and runoff. We thus modified the François and Walker (1992) parameterization for continental runoff by adding a factor proportional to the ratio of total oceanic versus continental area. Since the ocean basins increase during the sea-level rises (mainly through the extension of the epicontinental reservoirs), evaporation increases, and the model runoff is consequently enhanced. During sea-level fall episodes, the continental runoff tends to decrease.

(3) Sea-level changes may also affect the oceanic circulation. Sea-level rise episodes might result in the enhanced formation of warm saline deep waters in epicontinental seas, flowing back into the ocean, and finally stratifying it by reducing the vertical mixing (Brass et al., 1982). In order to test this hypothesis, we link the vertical mixing of the oceanic basins to sea level. The vertical mixing is assumed to decrease linearly with sea level during the sea-level rise episodes. We choose to cut completely the vertical mixing at the sea-level maxima to maximize the impacts of possible ocean stagnation during sea-level rises. In the simulations described below, we only apply the reduction of the vertical mixing to the Proto-Tethys basin. We also performed simulations where the vertical mixing was reduced in both the Panthalassa and Proto-Tethys oceans. However, this generally increases the disagreement between data and model output.

2.4. Calibration procedure

The weathering constants k_{sil}, k_{carb} and k_{SRC} are estimated using the temperature and runoff calculated for each latitude bands by the climate model under present-day conditions (1 PAL atmospheric CO_2, present-day continental configuration and present-day solar luminosity). k_{sil} is adjusted so that the present-day calculated consumption of CO_2 by silicate weathering reaches 11.7×10^{12} mol/yr (Gaillardet et al., 1999). k_{carb} is calibrated so that the global consumption of atmospheric CO_2 by carbonate weathering reaches 20.6×10^{12} mol/yr (Petsch and Berner, 1998) under present-day conditions, and k_{SRC} is fixed assuming that about 4.1×10^{12} mol/yr of O_2 are consumed by the oxidation of SRC (Petsch and Berner, 1998). The calibration of the oceanic and sediment submodel constants requires the calculation of the oceanic primary productivity, the recycling of organic matter within the water column, the deposition of carbonates. This calibration procedure cannot be performed with the COMBINE model in its Devonian configuration for two reasons. First, the configuration of the Devonian oceanic model differs from the configuration of the present-day oceans. Second, the COMBINE model in its Devonian version does not take into account the formation and subsequent deposition of carbonates in the open ocean. For these reasons, the ocean and sediment submodel constants were calibrated using a version of COMBINE fitted for present-day conditions (including carbonate formation in the open ocean, deep sea carbonate accumulation, one oceanic basin representing the global ocean, global circulation fitted to the Munhoven and François (1996) ocean box model). Once the ocean and sediment submodel constants fit so that DIC, alkalinity and oxygen gradients from the surface to the bottom waters are reproduced for the present-day conditions, these constants are exported into the COMBINE model in its Devonian version. The main parameters and calibration constants used in the COMBINE model and not listed in the text can be found in Table 1.

The COMBINE model (in its Devonian configuration) is then run for 20 million years with a global CO_2 degassing held constant at 4.5×10^{12} mol/yr (volcanic+mid-ocean ridge), and reaches a steady state that will be used as the pre-perturbation value. The atmospheric pCO_2 and pO_2 stabilize at 2925 ppm (10.5 times the present-day partial pressure) and 0.165 bar (0.66 times the present-day partial pressure), respectively. Given the range of uncertainties of the available reconstructions for these two variables, these values fall within an acceptable range. Global carbonate accumulation reaches 14.2×10^{12} mol/yr, 65% of it being deposited in the Proto-Tethys epicontinental area, the remaining 35% accumulating on the Panthalassa shelves. The burial of organic carbon

Table 1
Main parameters and calibration constants of the COMBINE model

Constant	Value	Reference
Continental silicate weathering constant k_{sil}	7.59×10^{-5} mol/l	calibrated from Gaillardet et al., 1999
Continental carbonate weathering k_{carb}	2.77×10^{-3} mol/l	calibrated from Petsch and Berner, 1998
SRC oxidation constant k_{SRC}	5.53×10^{-4} mol/l	calibrated from Petsch and Berner, 1998
Biotic carbonate accumulation constant k_d	0.172 mol/yr/m^2	François and Walker, 1992
C:P of buried organic matter under full oxic conditions	200 mol/mol	Van Cappellen and Ingall, 1996
C:P of buried organic matter under full anoxic conditions	4000 mol/mol	Van Cappellen and Ingall, 1996
Panthalassa surface	355×10^6 km^2	Estimated from Scotese and McKerrow, 1990
Proto-Tethys surface	53×10^6 km^2	Estimated from Scotese and McKerrow, 1990
Total continental surface	101.7×10^6 km^2	Estimated from Scotese and McKerrow, 1990
CO_2 air–sea exchange constant K_0	0.0572 mol/m^2/yr/μatm	Sarmiento et al., 1992
Devonian solar constant	1342.6 W/m^2	Endal and Sofia, 1981
$\delta^{13}C$ value of continental carbonate	+1‰ PDB	Holser et al., 1988
$\delta^{13}C$ value of continental SRC	−28‰ PDB	Hayes et al., 1999
$\delta^{13}C$ value of mantle carbon	−5‰ PDB	Holser et al., 1988
$\delta^{13}C$ value of aerial volcanic CO_2	−1‰ PDB	Mean value between the mid-ocean ridge and carbonate recycling, following the suggestion of Caldeira (1992)

equals 3.1×10^{12} mol/yr. The most favorable setting for the burial of organic carbon is the deep Proto-Tethys ocean seafloor, where 45% of the total burial of organic carbon occurs. The burial of organic carbon within the Panthalassa epicontinental reservoirs accounts for 42% of the total burial flux. The rest is buried on the deep Panthalassa seafloor, and within the epicontinental realm of the Proto-Tethys ocean.

3. Plausible scenarios and results

Given the number of processes and parameters included in the COMBINE model, the number of sensitivity tests that can be performed is almost unlimited. We choose to present only the simulations that illustrate the general behavior of the model, in response to the applied perturbations. All the following results show general trends that are not dependent on the values of the parameters at the first order, particularly on the pre-perturbation oceanic circulation. However, it should be kept in mind that the exact values of the model output are somewhat dependent on those parameters, particularly the regional distribution of the burial fluxes. But the general trends, spreading over several 10^5 to 10^6 years are not. Fig. 3 displays a brief schematic description of the tested hypotheses and the performed simulations.

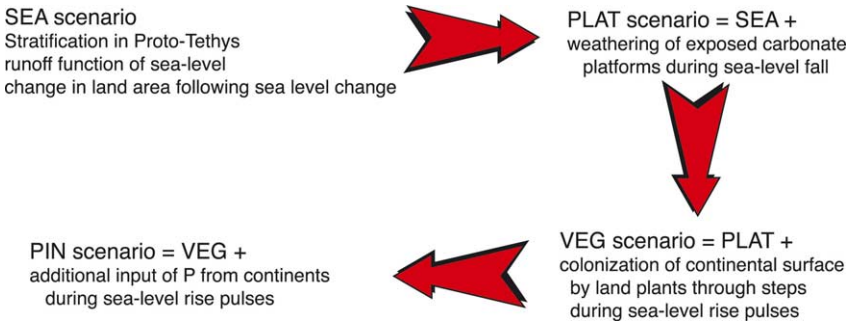

Fig. 3. A schematic view of the tested hypotheses and performed simulations.

3.1. The basic sea-level scenario

This first test is performed assuming all the above effects of sea-level change: continental area changes, modifications in the volume and surface of the oceanic basins, intensification of continental runoff during sea-level rise episodes, stagnation at the sea-level maxima within the Proto-Tethys ocean only, and decrease of continental runoff during sea-level fall. The calculated carbon isotope composition of the PTESE reservoir shows little change (Fig. 4e). During the sea-level rises, the PTESE $\delta^{13}C$ value remains roughly constant, while the carbon isotope composition of the PTESE decreases by about 0.15‰ during the Early Famennian fall in sea level. The model output disagrees with the observations. These minor changes in the carbon isotope signal are not driven by continental processes, since continental weathering fluxes remain almost unchanged during the simulation with increasing runoff compensating for the reduction in continental area during the sea-level rises and the decreasing runoff compensating for the increasing continental area during the Early Famennian sea-level fall. On the other hand, oceanic processes are heavily affected by the change in sea level. During both sea-level rises, the oxygen level in the Proto-Tethys deep epicontinental reservoir (PTEDE) declines within the dysoxic domain (Fig. 4c). The C:P value of buried organic matter below the PTEDE reservoir increases from 1000:1 to 2300:1 during the first sea-level rise, even reaching 3000:1 during the second sea-level fall. As a result, PO_4^{3-} concentration increases significantly within the PTEDE reservoir during the sea-level rises (Fig. 5).

However, the coeval calculated primary productivity within the Proto-Tethys surface reservoirs is reduced during the sea-level rises, since the upwelling of nutrients within the photic zone almost stops at the sea-level maximum. Despite a few percent increase in the primary productivity in the Panthalassa epicontinental surface reservoir

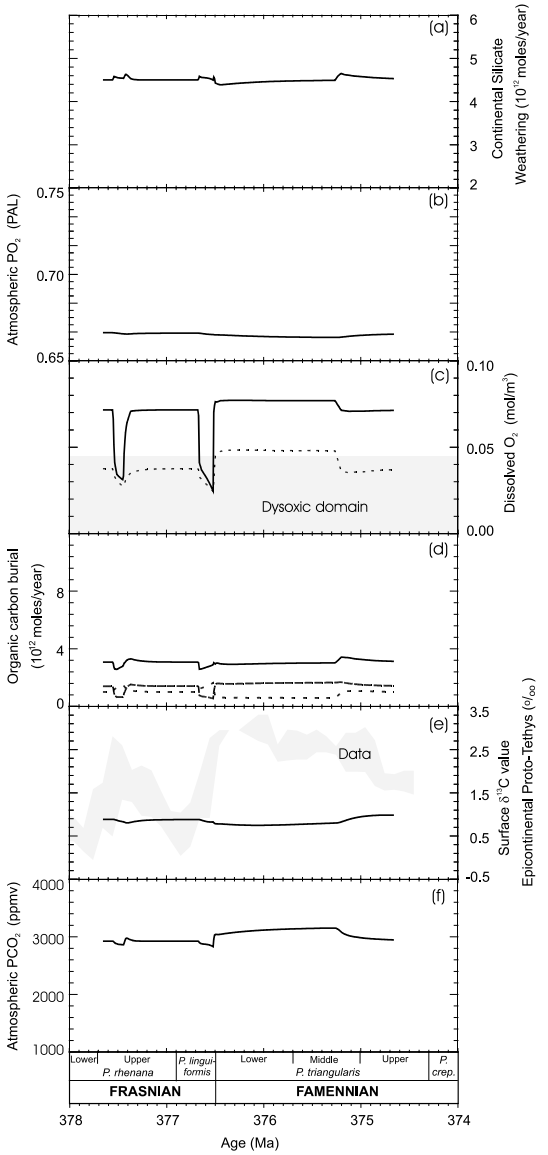

Fig. 4. Results of the SEA simulation (description in the text). (a) Global continental silicate weathering. (b) Atmospheric partial pressure of oxygen (in PAL). (c) Dissolved oxygen concentration; solid line: deep epicontinental Proto-Tethys reservoir (PTEDE), dotted line: deep epicontinental Panthalassa reservoir (PTADE); gray box: dysoxic domain. (d) Burial of organic carbon; dotted line: burial within the PTADE, dashed line: burial within the deep Proto-Tethys reservoir, solid line: total burial. (e) Calculated $\delta^{13}C$ values of dissolved CO_3^{2-} within the PTESE reservoir, compared to the available data. The shaded area includes 68% of the data around the moving average (± standard deviation around the mean for a Gaussian distribution of the data points). The moving average was run through the dataset with a step of 100 000 years, and a window width of 200 000 years. (f) Calculated atmospheric CO_2 partial pressure.

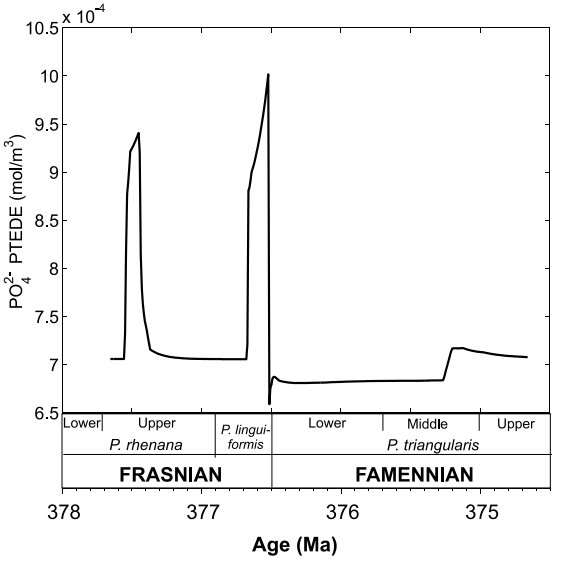

Fig. 5. PO_4^{3-} concentration within the PTEDE, as calculated by the SEA simulation.

(PTASE), the global productivity decreases by almost 10%. Globally, the amount of organic carbon reaching the sediment is thus reduced, but the conditions of preservation are improved by the developing dysoxia. As a result, the global flux of organic matter to the sediment displays a complex pattern, fluctuating rapidly during the sea-level rises, between 2.6×10^{12} and 3.3×10^{12} mol/year (starting from a pre-perturbation value of 3.1×10^{12} mol/year; Fig. 4d). This rather complex behavior is the result of the combination of the changes in the organic carbon burial flux within the different oceanic reservoirs. Regarding the main contributions to the global flux, the organic carbon burial flux increases by about 60% in the deep epicontinental area of the Panthalassa ocean (PTADE), but declines by 60% in the deep Proto-Tethys open reservoir (Fig. 4d). The combination of these changes is first a sudden but limited decrease of the total organic carbon burial, followed by a slow recovery back to pre-perturbation values covering the one million years of the Early Famennian sea-level fall (Fig. 4d).

Continental weathering fluxes are weakly perturbed by the Famennian sea-level fall (Fig. 4a for silicate weathering). The slow recovery of the organic carbon deposition flux together with a more or less constant SRC oxidation on continents results in a slow increase of the calculated seawater $\delta^{13}C$ value. Furthermore, the persisting disequilibrium between SRC oxidation and organic carbon deposition leads to an increase in atmospheric pCO_2, reaching 3150 ppmv at the end of the sea-level fall episode, and to a decrease in the atmospheric oxygen level by about 0.0027 PAL (Fig. 4f).

As a preliminary conclusion, the simulation shows that the impact of sea-level changes may have resulted in changes in oceanic circulation, runoff and geometry of the epicontinental reservoirs. However, this scenario cannot explain the variations in the carbon isotope composition recorded across the F-F boundary. The model suggests that the Early Famennian climate is warmed up due to increasing atmospheric pCO_2, and that atmospheric oxygen content declines while previous reconstructions suggest a rapid increase from the Late Devonian towards the Carboniferous (Berner, 2001).

3.2. Weathering of carbonate platforms

We modified the SEA scenario by introducing expected consequences of carbonate platform growth and erosion during sea-level rises and falls, respectively (PLAT simulation). The PLAT scenario can be seen as an application of sedimentary rapid recycling (Berner and Canfield, 1989) applied within the context of short-term isotopic excursions. During the two Frasnian sea-level rises, the model calculates the amount of carbonates deposited on the flooded part of the continents, and estimates their subsequent erosion once exposed to the atmosphere proportionally to the remaining mass of these platforms as a function of modelled climate (Eq. 3), in addition to the background continental flux. In terms of the carbon and alkalinity budgets, the sea-level rise episodes have very little impact on the geochemical cycles, because they are short and limited in amplitude. The maximum carbonate mass deposited during the sea-level rises is calculated to be 0.5×10^{18} mol carbon. The impact on seawater $\delta^{13}C$ value is extremely small, since the carbonates were deposited in isotopic equilibrium with coeval

seawater, their subsequent erosion having a very minor impact on the oceanic $\delta^{13}C$ budget. On the other hand, the Famennian sea-level fall might have had a major impact on the seawater $\delta^{13}C$ composition, since older carbonates with $\delta^{13}C$ values different from the Late Frasnian mean oceanic value may have been exposed during a relatively long period (1.5 million years). Because the uppermost part of these platform carbonates will be of Devonian age, we assume that the mean $\delta^{13}C$ value of carbon released by chemical weathering of these carbonates can be approximated by an average carbon isotopic composition of +1.5‰ PDB (Veizer et al., 1999). Estimating the actual surface of exposed carbonates during the sea-level fall is not possible. Again, in order to identify the maximum possible impact, we will assume that all continental margins exposed during the sea-level fall (below the pre-perturbation sea level) are covered by Devonian carbonates. This assumption implies that the increase of continental area during the sea-level fall affected neither silicate nor kerogen carbon weathering.

As expected, the response of the ocean–atmosphere system is similar to the results of the SEA simulation for the Frasnian (Fig. 6). The sea-level fall observed during the earliest Famennian results in the exposure and weathering of Devonian carbonates consuming atmospheric CO_2 at a calculated maximum rate of 4.7×10^{12} mol/year. The model assumes that carbonates contain P at a C:P ratio of 1000:1 (Froelich et al., 1982). The weathering of the carbonate platforms exposed by the sea-level fall thus implies an increase in the delivery of continental phosphorus to the ocean by 4.7×10^{9} mol/year, representing a 17% increase of the continental phosphorus flux relative to the coeval SEA scenario value. The consequence is an enhanced primary productivity within the Proto-Tethys photic zone and consequently an enhanced organic carbon burial flux in the Proto-Tethys basin, reaching up to 2.0×10^{12} mol/year (compared to the pre-perturbation value of 1.5×10^{12} mol/year; Fig. 6d). On the other hand, oxygenation of the epicontinental deep reservoirs (due to the decrease in size of these reservoirs during the sea-level fall) leads to a decreased preservation of organic matter within the epicontinental sedimentary layer. This effect is comparable in magnitude to the SEA simulation (Fig. 6c). The net effect is a global burial flux of organic carbon which is in excess by about 0.4×10^{12} mol/year compared to the production of carbon by continental kerogen weathering for about one million years (covering the sea-level fall episode).

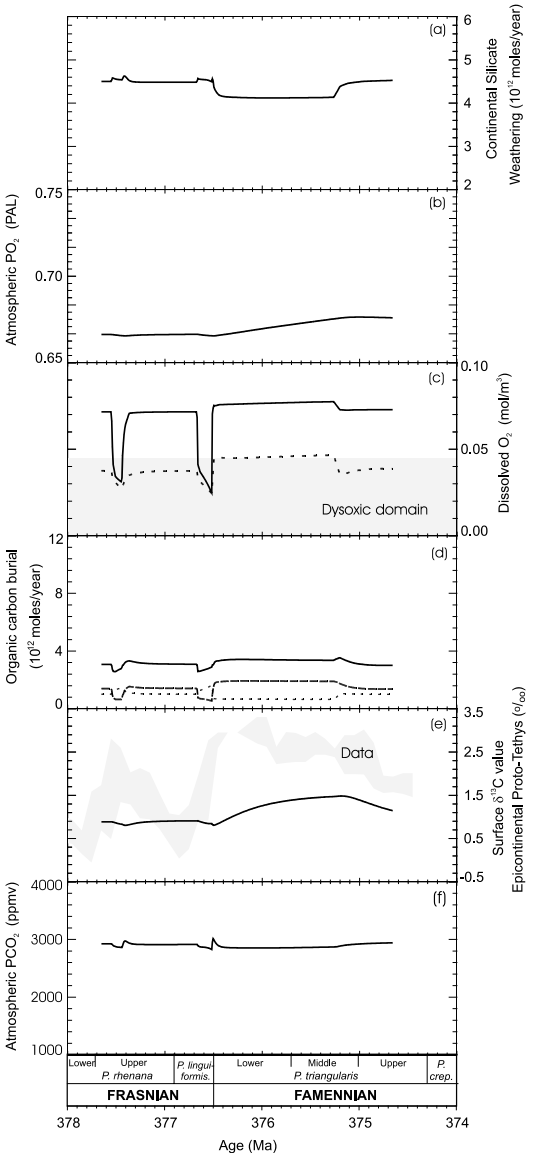

Fig. 6. Results of the PLAT simulation (description in the text). See caption of Fig. 4 for more details.

As a result of this disequilibrium, atmospheric

oxygen increases from 0.665 PAL at the F-F boundary to 0.676 PAL at the end of the sea-level fall episode (Fig. 6b). Atmospheric CO_2 is weakly influenced, despite the fact that the organic carbon subcycle acts as a global sink of carbon (carbon sink being larger than the source; Fig. 6f). However, the additional continental area exposed during the sea-level fall episode is covered by carbonates in this simulation. As a consequence, the decrease of the consumption of atmospheric CO_2 by continental silicate weathering due to the decrease in runoff (linked to a drier climate during the sea-level fall episode) is not compensated by an increase in the area of exposed silicate rocks. The decrease in silicate weathering (Fig. 6a) leads to an increasing pCO_2 at assumed constant mid-ocean ridge and volcanic CO_2 degassing rates, counteracting the sink due to the enhanced burial of organic matter.

In addition, the modelled PTESE $\delta^{13}C$ data display a comparable pattern (minor negative excursion in $\delta^{13}C$ value) during the two sea-level rise events. The Early Famennian sea-level fall is characterized by a +0.7‰ excursion lasting about 1 million years, which is in better agreement with measured $\delta^{13}C$ values (Fig. 6e). The causes of this excursion are twofold: (1) the calculated weathering of the carbonate platform directly injects relatively heavy carbon ($\delta^{13}C = 1.5$‰) into the ocean; (2) the phosphorus supplied by the weathering of carbonates enhances the productivity in surface waters, and the organic carbon deposition flux. It should be noted that in terms of $\delta^{13}C$ values the response of the various oceanic surface reservoirs (epicontinental or open ocean) is almost identical. The carbon reservoir of each oceanic surface reservoir 'interacts' with atmospheric CO_2 through gas exchange, tending to homogenize the isotopic ratios of surface waters. Small differences (0.4‰ maximum) are due to differences in temperature in the various surface reservoirs, and to changes in productivity. However, even if the agreement between the calculated and measured $\delta^{13}C$ data is improved, the model suggests that the maximum effect of carbonate platform weathering is not sufficient to account for the high $\delta^{13}C$ values measured during the Early Famennian.

Carbonate platform weathering has been invoked by Kump et al. (1999) in order to explain a +6‰ excursion in carbonate carbon isotope composition during the Late Ordovician. In their study, the authors argue that such a prominent excursion in the $\delta^{13}C$ values might be produced by changing the relative contribution of carbonate versus organic carbon weathering. Increasing the fraction of carbon derived from carbonate weathering in the total riverine carbon flux from 72% to 96% is thought to be sufficient to increase seawater $\delta^{13}C$ value by 6‰. However, Kump et al. (1999) keep the global flux of riverine carbon constant, so that their suggested increase in the carbonate contribution implies a proportional decrease in the carbon flux from the oxidation of sedimentary organic carbon, which has an important impact on the seawater $\delta^{13}C$ value. In the present work, the 50% enhanced carbonate weathering increases seawater $\delta^{13}C$ value by only 0.7‰. Indeed, the global riverine carbon flux from the oxidation of continental sedimentary organic carbon together with the contribution from carbonate weathering increases widely during the sea-level fall. As a consequence, the impact of carbonate weathering on the carbon isotopic budget of the ocean might be much smaller than suggested by Kump et al. (1999).

3.3. Colonization of continental surfaces by land plants

Algeo et al. (1995) and Algeo and Scheckler (1998) suggested that the rapid colonization of drier upland areas by higher plants during the Late Devonian might explain the sedimentation of organic carbon-rich Late Devonian black shales and the observed excursions in carbonate $\delta^{13}C$ values. The development of soils and microbial activities as a consequence of the colonization by land plants may have affected local weathering, resulting in a global enhancement of the weatherability of continental surfaces (weatherability is defined as the product of factors that affect chemical erosion other than climate change; Kump and Arthur, 1997). Mathematically, this enhanced weatherability translates into the increase of the f_e factor in Eqs. 1 and 3. f_e increases

by a factor of 5, if a non-vegetated area becomes covered by vascular plants (gymnosperms; Berner, 1994). Furthermore, the dependence of chemical weathering on atmospheric CO_2 will change (Eq. 2), due to the concentration of atmospheric CO_2 in soils by plant roots and microbes (Berner, 1994).

The overall effect of the colonization of continental surfaces by land plants is thus an increase in global chemical weathering. As a result, pCO_2 will decrease, since the enhanced weathering will consume CO_2. After a few million years (several times the residence time of carbon in the ocean–atmosphere system), the atmospheric pCO_2 will reach a new steady-state value, which will be lower than the initial concentration. If volcanic degassing was constant during the transition, the delivery of nutrients by continental chemical weathering will be the same prior to and after the colonization event. However, during the transition from a high to a low steady-state pCO_2, the flux of dissolved materials transferred from the continents to the ocean will first increase rapidly, and then decrease towards its pre-perturbation value. This non-equilibrium situation will result in an enhanced delivery of nutrients to the ocean, stimulate oceanic productivity, and potentially reinforce anoxic conditions in the deeper part of the epicontinental and open oceans.

However, two questions remain to be answered: (1) Does the spreading of vascular plants increase global weatherability? This question is fully debated in a recent review paper by Boucot and Gray (2001). The authors emphasize that, even if the development of higher plants initially intensified chemical weathering, the efficiency of this process will decrease through time as soils accumulate over the bedrock, limiting the circulation of water. The effect of higher plants on chemical weathering might only be efficient on a long time scale if mechanical erosion regularly removes the soil cover. In the particular case of the Late Devonian time period, we feel that the colonization of the continents by land plants will result in an enhancement of the weatherability of the continental surface for at least several 10^5 to 10^6 years, prior to the development of thick soils. As an example, Tardy (1993) calculated that it takes about 330 000 years to develop a 1 m thick soil horizon in a tropical environment characterized by a precipitation of 800 mm/yr. Furthermore, as will be discussed below from model simulations, the Early Famennian is a period of long-term climatic cooling, an evolution that will reduce the extension of warm tropical climatic belts, and finally enhance mechanical weathering. For these two reasons, we argue that the hypothesis of Algeo and Scheckler (1998) might be a relevant process to increase the delivery of nutrients to the oceans. (2) The second question is one of timing. Is there any connection between the Late Frasnian sea-level rises and the colonization of continental area by vascular plants? Is it possible that a sea-level rise leading to increased moisture over continents triggered a rapid colonization of dry uplands by land plants during this period of intense and rapid plant evolution?

We tested such a hypothetical scenario (VEG simulation). Starting from a vegetation (vascular plants) that covered 10% of the continental area during the Frasnian in the PLAT scenario, we superimpose a 5% increase of the continental vegetated area triggered by the first sea-level rise, and a further 25% increase during the second sea-level rise. This colonization is assumed to be equally distributed between all latitude bands. These numbers were chosen firstly to allow us to explore the impact of minor and major spreading of vascular plants, and secondly since they represent the best a posteriori combination to fit the calculated seawater $\delta^{13}C$ value with the data. Both colonization events start at the onset of the sea-level rises. The colonization events occur instantaneously (at geological time scales), but f_e and FCO_2 for the new vegetated areas change linearly over 50 000 years from non-vegetated values ($f_e = 0.15$) to fully vegetated values ($f_e = 0.75$; Berner, 1994). This delay roughly accounts for the time required for the development of new soils.

The impact on the calculated evolution of atmospheric CO_2 pressure is drastic (Fig. 7f). During the first sea-level rise, pCO_2 first declines from 2925 to about 2730 ppmv. A further decrease to about 2540 ppmv is observed just prior to the onset of the second sea-level rise (this change cor-

responds to an overall change in mean global temperature of about 0.5°C). The effect of the second sea-level rise, combined with a 25% increase in plant cover, is a global pCO_2 decrease of about 1000 ppmv, which corresponds to an additional global cooling of more than 2°C, reached about 1 million years after the F-F boundary. pCO_2 then remains constant, having

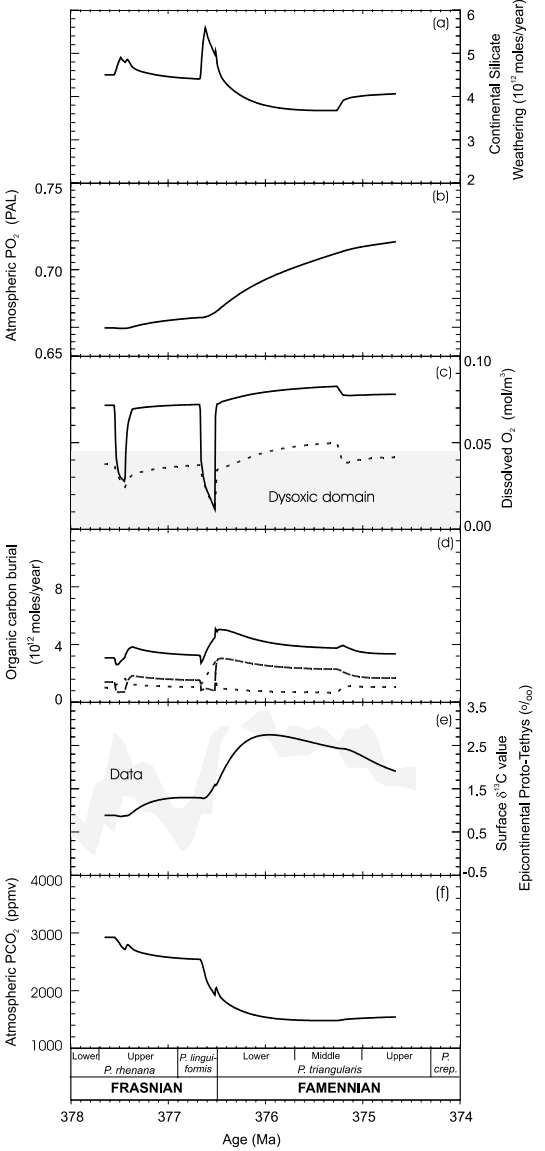

Fig. 7. Results of the VEG simulation (description in the text). See caption of Fig. 4 for more details.

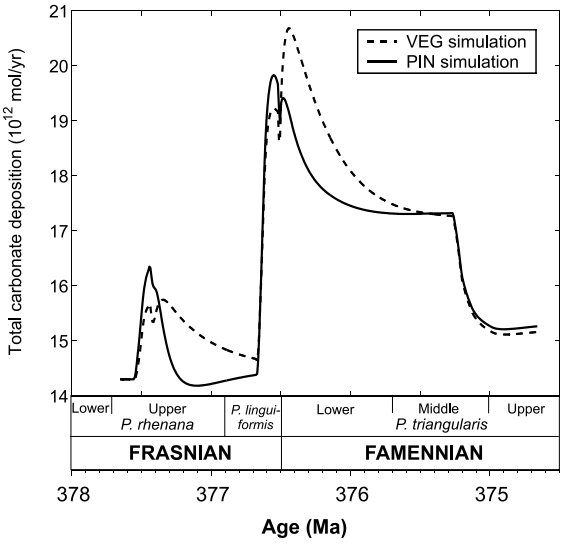

Fig. 8. Total carbonate deposition calculated by the VEG and PIN simulations.

reached a new steady state. The reason for the enduring decrease in atmospheric CO_2 well after the sea-level rises is due to the increase of the continental phosphorus delivery as a consequence of the spreading of land plants. Since this flux is assumed to be not directly dependent on temperature (Eq. 3), it is less sensitive to the ongoing global climatic cooling than the global silicate weathering flux. Due to the increase of nutrient supply, productivity in surface waters and consequently organic carbon burial are strongly enhanced (Fig. 7d) during more than 1 Myr after the colonization events.

The two sea-level rises and colonization events result in an increase of the PTESE $\delta^{13}C$ value by 0.4‰ and 1.4‰, respectively (Fig. 7e). The Famennian $\delta^{13}C$ value plateau is now well reproduced by combining the effect of carbonate platform weathering and spreading of land plants. However, there is a 500 000-year delay between the onset of the colonization event and the maximum excursion in the PTESE carbon isotope values, because of the residence time of carbon in the ocean–atmosphere system. Finally, the atmospheric oxygen concentration increases by about 0.05 PAL (2.0×10^{18} mol) over 3 million years due to the increasing burial of organic matter (Fig. 7b). Atmospheric oxygen has not yet reached a

steady state at the end of the simulation, and will probably increase for an additional 2 million years. The carbonate accumulation flux displays a major increase during the Early Famennian, following the increased delivery of alkalinity into the oceans related to the increased weatherability of the continents and weathering of carbonates during the sea-level fall (Fig. 8).

3.4. Continental phosphorus required

Finally, we used the COMBINE model in a reverse mode. The two main disagreements between calculated seawater $\delta^{13}C$ values by the VEG simulation and measured $\delta^{13}C$ values are observed in the Upper *rhenana* conodont Zone (the model almost does not produce an isotopic excursion), and at the F-F boundary (the calculated rate of increase in $\delta^{13}C$ value is too gradual in comparison to the measured data; Fig. 7e). By adding to the VEG simulation an arbitrary process in order to reproduce the fluctuations in seawater $\delta^{13}C$ value, the model will calculate an atmospheric pCO_2 and a climate in agreement with the available $\delta^{13}C$ isotope data. However, the reverse mode will not give any information about the cause of these perturbations.

A convenient way to produce excursions in seawater $\delta^{13}C$ value is to perturb the organic carbon subcycle, since the $\delta^{13}C$ value of the organic matter is largely different from the mean seawater $\delta^{13}C$ value. Assuming that the Frasnian excursions are linked to the sea-level rises, we simply add a continental phosphorus flux proportionally to the change in sea level (PIN simulation). Such additional P flux facilitates the onset of dysoxic conditions during the sea-level rises by increasing the primary productivity within epicontinental surface waters. Starting from the VEG simulation, we found that an additional flux of 8.0×10^9 mol/year of phosphorus (40% increase compared to the pre-perturbation Devonian flux) to the VEG scenario is required at the sea-level maxima to account for the observed shift in the carbon isotope composition, and to match the sharp increase in the $\delta^{13}C$ values at the F-F boundary (Fig. 9e). Since the COMBINE model is now working in a reverse mode, the origin of this

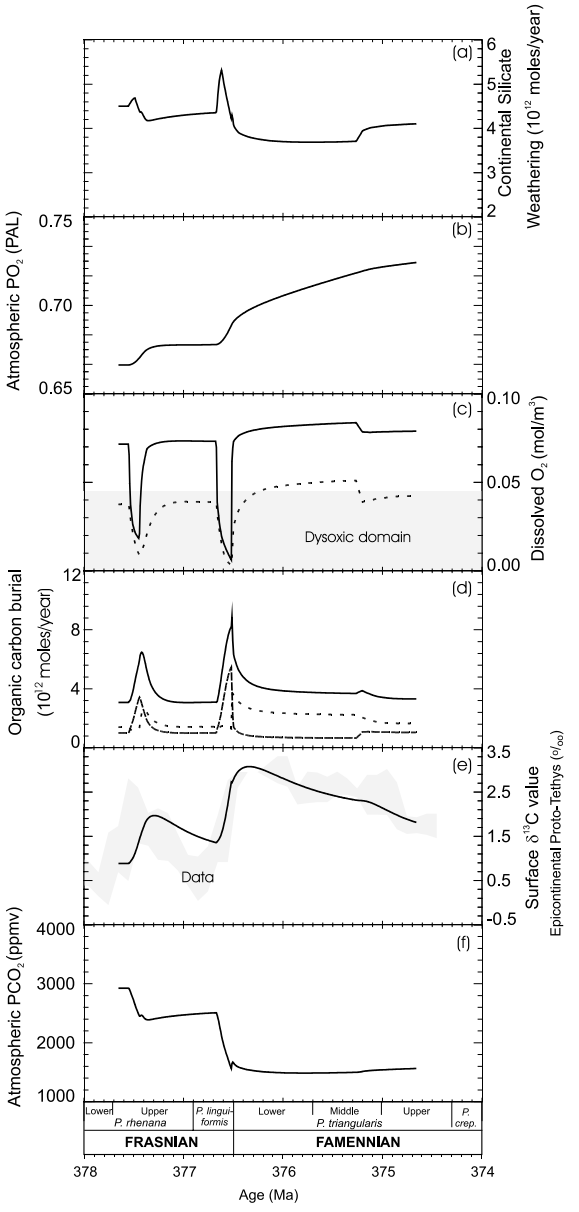

Fig. 9. Results of the PIN simulation (description in the text). See caption of Fig. 4 for more details.

flux cannot be deduced from the simulation itself. We can only speculate on the origin of this flux which could be an influx of nutrients from flooded lagoons as a consequence of the rise in sea level (Racki, 1993). However, once the PTESE $\delta^{13}C$ values are reproduced, we have some confidence in the output of the model describing the

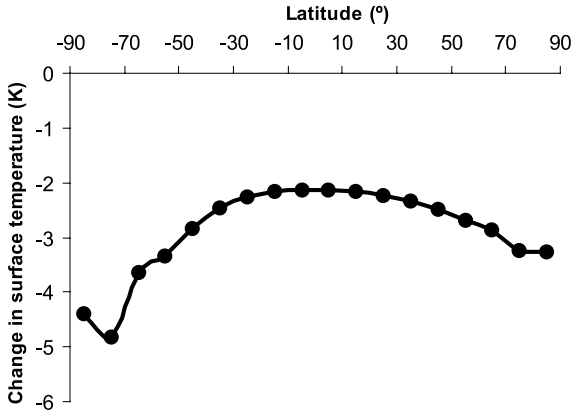

Fig. 10. Difference in surface temperature between the Upper *triangularis* and Lower *rhenana* conodont Zones as a function of latitude, as calculated by the PIN simulation.

geochemical cycles of carbon, oxygen and phosphorus.

With this model, atmospheric pCO_2 declines during both sea-level rises by 530 ppmv and 940 ppmv, respectively. Atmospheric CO_2 concentrations remain constant during the Early Famennian (Fig. 9f). The overall decline in global mean temperature across the F-F boundary equals 2.7°C (4.4°C at the south pole, 2.1°C at the equator; Fig. 10). The Panthalassa and Proto-Tethys epicontinental seas experience dysoxic conditions during the sea-level rise, essentially due to the intensified productivity in surface waters driven by the enhanced continental nutrient supply and a coeval sluggish vertical mixing. As a consequence, the organic carbon burial increases during the sea-level rise events reaching more than 9×10^{12} mol/year at the sea-level maxima, a value three times higher than the pre-perturbation Frasnian value (Fig. 9d). Atmospheric oxygen now displays two stepwise increases during the Kellwasser event (about 4×10^{17} mol oxygen are added to the atmospheric reservoir during both events), followed by a slower increase related to the spreading of land plants (VEG simulation; Fig. 9b). The model predicts a rapid and short-lived increase in the carbonate deposition rate during the sea-level rise events, essentially related to decreasing atmospheric pCO_2, leading to less acidic conditions in epicontinental seas (Fig. 8).

4. Conclusions

This study demonstrates the complexity of interpreting the short-term excursions in $\delta^{13}C$ values observed in the Late Frasnian and earliest Famennian. Various scenarios were tested in order to reproduce the measured $\delta^{13}C$ values across the F-F boundary using the COMBINE model, which is a model of the global biogeochemical cycles fully coupled to an energy-balance climate model. A scenario exclusively based on oceanic processes fails to generate dysoxic conditions below 100 m in epicontinental seas and an increase in organic carbon deposition. There is an unresolved paradox between the requirement of a stratified ocean to produce anoxia, and the requirement of a sustained biological productivity within the photic zone of the ocean to ensure the production and subsequent preservation of large quantities of organic carbon in the sediments (strong productivity in the photic zone requires the existence of strong upwelling). By stratifying the ocean during the sea-level rises as a result of the perturbation of the ocean vertical mixing through the formation of warm saline deep waters in extended epicontinental seas, we produced widespread anoxia, but no excursion in seawater $\delta^{13}C$ values as well as no significant change in atmospheric pCO_2.

However, we demonstrate the importance of the three continental processes in generating the short-term carbon isotope excursions in the Late Frasnian and Early Famennian.

(1) The weathering of carbonate platform exposed during the Early Famennian sea-level fall might account for a maximum +0.7‰ positive shift in seawater $\delta^{13}C$ values.

(2) The potential rapid spreading of land plants across the F-F transition, through the colonization of about 30% of the continental surface, accounts for a further +1.0‰ positive shift in $\delta^{13}C$ during the Early Famennian. The change in continental weatherability results in the consumption of 1400 ppmv of atmospheric CO_2 across the boundary. The Early Famennian climate is calculated to be 2.7°C cooler than the Late Frasnian climate (4.4°C at the pole, and 2.1°C at the equator), in agreement with various sedimentological

and isotopic constraints (Streel et al., 2000; Joachimski and Buggisch, 2002). However, because of residence time consideration, such a scenario cannot explain the short-lived excursion in the carbon isotope composition in the Upper *rhenana* conodont Zone and the rapid increase in the $\delta^{13}C$ values in the latest Frasnian.

(3) These rapid positive shifts in the carbon isotope composition require an increase in the phosphorus flux from the continent by about 40% during the sea-level rises and coeval ocean stagnation, to sustain productivity in the photic zone. This additional phosphorus flux possibly originated from flooded lagoons (Racki, 1993). As a result, the total burial of organic carbon increases by a factor of 2 to 3 during the sea-level rises. This organic carbon is accumulated under dysoxic conditions, and results in the formation of the two Kellwasser horizons. The oxygen content of the atmosphere consequently increases by more than 2.20×10^{18} mol (0.06 PAL) across the F-F boundary, leading to a better oxygenation of the oceanic reservoirs in the Famennian compared to the Frasnian.

Acknowledgements

Guy Munhoven and Louis M. François at the LPAP (Liège) are greatly acknowledged for stimulating discussions about the model structure. We thank Kevin Faure and an anonymous reviewer for constructive comments and for improving the readability of this contribution. We thank Finn Surlyk for valuable comments.

References

Algeo, T.J., Berner, R.A., Maynard, J.B., Scheckler, S.E., 1995. Late Devonian oceanic anoxic events and biotic crises: 'rooted' in the evolution of vascular land plants? Geol. Soc. Am. Today 5, 63–66.

Algeo, T.J., Scheckler, S.E., 1998. Terrestrial-marine teleconnections in the Devonian: links between the evolution of land plants, weathering processes, and marine anoxic events. Phil. Trans. R. Soc. London B 353, 113–130.

Anderson, L.A., Sarmiento, J.L., 1994. Redfield ratio of remineralization determined by nutrient data analysis. Global Biogeochem. Cycles 8, 65–80.

Benitez-Nelson, C.R., 2000. The biogeochemical cycling of phosphorus in marine systems. Earth Sci. Rev. 51, 109–135.

Berner, R.A., 1994. GEOCARB II: a revised model for atmospheric CO_2 over Phanerozoic time. Am. J. Sci. 294, 56–91.

Berner, R.A., 2001. Modeling atmospheric O_2 over Phanerozoic time. Geochim. Cosmochim. Acta 65, 685–694.

Berner, R.A., Canfield, D.E., 1989. A new model for atmospheric oxygen over Phanerozoic time. Am. J. Sci. 289, 333–361.

Berner, R.A., Petsch, S.T., Lake, J.A., Beerling, D.J., Popp, B.N., Lane, R.S., Laws, E.A., Westley, M.B., Cassar, N., Woodward, F.I., Quick, W.P., 2000. Isotope fractionation and atmospheric oxygen: implications for the Phanerozoic O_2 evolution. Science 287, 1630–1633.

Boucot, A.J., Gray, J., 2001. A critique of Phanerozoic climatic models involving changes in the CO_2 content of the atmosphere. Earth Sci. Rev. 56, 1–159.

Brady, P.V., 1991. The effect of silicate weathering on global temperature and atmospheric CO_2. J. Geophys. Res. 96, 18101–18106.

Brass, G.W., Southam, J.R., Peterson, W.H., 1982. Warm saline bottom water in the ancient ocean. Nature 296, 620–623.

Buggisch, W., 1991. The global Frasnian-Famennian 'Kellwasser event'. Geol. Rundsch. 80, 49–72.

Caldeira, K., 1992. Enhanced Cenozoic chemical weathering and the subduction of pelagic carbonates. Nature 357, 578–581.

Copper, P., 1977. Paleolatitudes in the Devonian of Brazil and the Frasnian-Famennian extinction event. Palaeogeogr. Palaeoclimatol. Palaeoecol. 21, 165–207.

Copper, P., 1986. Frasnian/Famennian mass extinction and cold-water oceans. Geology 14, 835–839.

Deines, P., 2002. The carbon isotope geochemistry of mantle xenoliths. Earth Sci. Rev. 58, 247–278.

Endal, A.S., Sofia, S., 1981. Rotation in solar-type stars, I, Evolutionary models for the spin-down of the Sun. Astrophys. J. 243, 625–640.

François, L.M., Walker, J.C.G., 1992. Modelling the Phanerozoic carbon cycle and climate: constraints from the $^{87}Sr/^{86}Sr$ isotopic ratio of seawater. Am. J. Sci. 292, 81–135.

François, L.M., Goddéris, Y., 1998. Isotopic constraints on the Cenozoic evolution of the carbon cycle. Chem. Geol. 145, 177–212.

Freeman, K.H., Hayes, J.M., 1992. Fractionation of carbon isotopes by phytoplankton and estimates of ancient CO_2 levels. Global Biogeochem. Cycles 6, 185–198.

Froelich, P.N., Bender, M.L., Luedtke, N.A., 1982. The marine phosphorus cycle. Am. J. Sci. 282, 474–511.

Gaillardet, J., Dupré, B., Louvat, P., Allègre, C.J., 1999. Global silicate weathering and CO_2 consumption rates deduced from the chemistry of large rivers. Chem. Geol. 159, 3–30.

Goddéris, Y., 1997. Modélisation de l'évolution cénozoïque des cycles biogéochimiques: impact de l'orogenèse himalayenne. Thèse de doctorat, Faculté des Sciences, Université de Liège, Liège.

Goddéris, Y., François, L.M., 1995. The Cenozoic evolution

of the strontium and carbon cycles: relative importance of continental erosion and mantle exchange. Chem. Geol. 126, 169–190.

Goddéris, Y., François, L.M., 1996. Balancing the Cenozoic carbon and alkalinity cycles: constraints from isotopic records. Geophys. Res. Lett. 23, 3743–3746.

Goddéris, Y., Veizer, J., 2000. Tectonic control of chemical and isotopic composition of ancient oceans: the impact of continental growth. Am. J. Sci. 300, 434–461.

Hallam, A., Wignall, P.B., 1997. Mass Extinctions and Their Aftermath. Oxford University Press, Oxford.

Hayes, J.M., Strauss, H., Kaufman, A.J., 1999. The abundance of 13C in marine organic matter and isotopic fractionation in the global biogeochemical cycle of the carbon during the past 800 Ma. Chem. Geol. 161, 103–125.

Holser, W.T., Schidlowski, M., McKenzie, F.T., Maynard, J.B., 1988. Geochemical cycles of carbon and sulfur. In: Gregor, C.B., Garrels, R.M., McKenzie, F.T., Maynard, J.B. (Eds.), Chemical Cycles in the Evolution of the Earth. Wiley, New York, pp. 105–173.

Joachimski, M., Buggisch, W., 1993. Anoxic events in the Late Frasnian – causes of the Frasnian–Famennian faunal crisis? Geology 21, 675–678.

Joachimski, M., Ostertag-Henning, C., Pancost, R.D., Strauss, H., Freeman, K.H., Littke, R., Sinninghe Damsté, J.S., Racki, G., 2001. Water column anoxia, enhanced productivity and concomitant changes in $\delta^{13}C$ and $\delta^{34}S$ across the Frasnian–Famennian boundary (Kowala-Holy Cross Mountains/Poland). Chem. Geol. 175, 109–131.

Joachimski, M.M., Pancost, R.D., Freeman, K.H., Ostertag-Henning, C., Buggisch, W., 2002. Carbon isotope geochemistry of the Frasnian–Famennian transition. Palaeogeogr. Palaeoclimatol. Palaeoecol. 181, 91–109.

Joachimski, M.M., Buggisch, W., 2002. Conodont apatite $\delta^{18}O$ signatures indicate climatic cooling as a trigger of the Late Devonian (F-F) mass extinction. Geology 30, 711–714.

Johnson, J.G., Klapper, G.S., Sandberg, C.A., 1985. Devonian eustatic fluctuations in Euramerica. Geol. Soc. Am. Bull. 96, 567–587.

Kump, L.R., Arthur, M.A., 1997. Global chemical erosion during the Cenozoic: weatherability balances the budgets. In: Ruddiman, W.F. (Ed.), Tectonic Uplift and Climate Change. Plenum Press, New York, pp. 399–426.

Kump, L.R., Arthur, M.A., 1999. Interpreting carbon-isotope excursions: carbonates and organic matter. Chem. Geol. 161, 181–198.

Kump, L.R., Arthur, M.A., Patzkowsky, M.E., Gibbs, M.T., Pinkus, D.S., Sheehan, P.M., 1999. A weathering hypothesis for glaciation at high atmospheric pCO_2 during the Late Ordovician. Palaeogeogr. Palaeoclimatol. Palaeoecol. 152, 173–187.

McGhee, G.R., 2001. The 'multiple impacts hypothesis' for mass exctinction: a comparison of the Late Devonian and the Late Eocene. Palaeogeogr. Palaeoclimatol. Palaeoecol. 176, 47–58.

McLaren, D.J., 1970. Time, life, and boundaries. J. Paleontol. 44, 801–815.

Mook, W.G., Bommerson, J.C., Staverman, W.H., 1974. Carbon isotope fractionation between dissolved and gaseous carbon dioxide. Earth Planet. Sci. Lett. 22, 169–176.

Munhoven, G., 1997. Modeling Glacial-Interglacial Atmospheric CO_2 Variations: The Role of Continental Weathering. PhD Thesis, University of Liège, Liège.

Munhoven, G., François, L.M., 1996. Glacial-interglacial variability of atmospheric CO_2 due to changing continental silicate rock weathering: a model study. J. Geophys. Res. 101, 21423–21437.

Murphy, A.E., Sageman, B.B., Hollander D.J., Lyons, T.W., 2000. Black shale deposition and faunal overturn in the Devonian Appalachian basin: clastic starvation, seasonal water-column mixing, and efficient biolimiting nutrient recycling. In: Huber, B.T., MacLeod, K.G., Wing, S.L. (Eds.), Warm Climates in Earth History. Cambridge University Press, Cambridge, pp. 351–385.

Opdyke, B.N., Wilkinson, 1988. Surface area control of shallow cratonic to deep marine carbonate accumulation. Paleoceanography 3, 685–703.

Ormiston, A.R., Oglesby, R.J., 1995. Effect of Late Devonian paleoclimate on source rock quality and location. Am. Assoc. Pet. Geol. Stud. Geol. 40, 105–132.

Petsch, S., Berner, R.A., 1998. Coupling the geochemical cycles of C, P, Fe, and S: the effect on atmospheric O_2 and the isotopic records of carbon and sulfur. Am. J. Sci. 298, 246–262.

Racki, G., 1993. Evolution of the bank to reef complex in the Devonian of the Holy Cross mountains. Acta Palaeontol. Pol. 37, 87–182.

Racki, G., 1998. Frasnian–Famennian biotic crisis: underevaluated tectonic control? Palaeogeogr. Palaeoclimatol. Palaeoecol. 141, 177–198.

Sandberg, C.S., Ziegler, W., 1996. Devonian conodont biochronology in geologic time calibration. Senckenb. Lethaea 76, 259–265.

Sarmiento, J.L., Orr, J.C., Siegenthaler, U., 1992. A perturbation simulation of CO_2 uptake in an ocean general circulation model. J. Geophys. Res. 97, 3621–3645.

Scotese, C.R., McKerrow, W.S., 1990. Revised world map and introduction. In: McKerrow, W.S., Scotese, C.R. (Eds.), Paleozoic Paleogeography and Biogeography. Geol. Soc. London Mem. 51, 1–21.

Siegenthaler, U., Münnich, K.O., 1981. $^{13}C/^{12}C$ fractionation during CO_2 transfer from air to sea. In: Bolin, B. (Ed.), Carbon Cycle Modeling. John Wiley and Sons, Chichester, pp. 249–257.

Streel, M., Caputo, M.V., Loboziak, S., Melo, J.H.G., 2000. Late Frasnian–Famennian climates based on palynomorph analyses and the question of the Late Devonian glaciations. Earth Sci. Rev. 52, 121–173.

Tardy, Y., 1993. Climats, paléoclimats et biogéodynamique du paysage tropical. In: Paquet, H., Clauer, N. (Eds.), Compterendu du colloque 'Sédimentologie et géochimie de la surface' à la mémoire de G. Millot. Colloque de l'Académie des Sciences et du CADAS, Paris.

Thompson, J.B., Newton, C.R., 1988. Late Devonian mass

extinction: Episodic climatic cooling or warming. In: McMillian, N.J., Embry, A., Glass, D.J. (Eds.), Devonian of the World. Can. Soc. Petrol. Mineral. Mem. 14, pp. 29–34.

Tucker, R.D., Bradley, D.C., Ver Straeten, C.A., Harris, A.G., Ebert, J.R., McCutcheon, S.R., 1998. New U–Pb zircon ages and the duration and division of Devonian time. Earth Planet. Sci. Lett. 158, 175–186.

Van Cappellen, P., Ingall, E.D., 1996. Redox stabilization of the atmosphere and oceans by phosphorus-limited marine productivity. Science 271, 493–496.

Veizer, J., Ala, D., Azmy, K., Bruckschen, P., Buhl, D., Bruhn, F., Carden, G.A.F., Diener, A., Ebneth, S., Goddéris, Y., Jasper, T., Korte, C., Pawellek, F., Podlaha, O.G., Strauss, H., 1999. $^{87}Sr/^{86}Sr$, $\delta^{13}C$ and $\delta^{18}O$ evolution of Phanerozoic seawater. Chem. Geol. 161, 59–88.

Veizer, J., Goddéris, Y., François, L.M., 2000. Evidence for decoupling of atmospheric CO_2 and global climate during the Phanerozoic eon. Nature 408, 698–701.

Wallmann, K., 1999. Die Rolle der Subduktionszonen im globalen Wasser- und Kohlenstoffkreislauf. Habilitationsschrift, University of Kiel, Kiel.

Wanninkof, R., 1992. Relationship between wind speed and gas exchange over the ocean. J. Geophys. Res. 97, 7373–7382.